

Euler-modified pulley-type microring on lithium niobate platform

Wen-Hui Song(宋文慧), Dong-Jie Guo(郭东洁), Ran Yang(杨然), Jia-Chen Duan(端家晨), Zi-Shuo Gu(顾子硕), Ji Tang(汤济), Zhilin Ye(叶志霖), Xiao-Hui Tian(田晓慧), Kunpeng Jia(贾琨鹏), Zhong Yan(严仲), Zhijun Yin(尹志军), Yan-Xiao Gong(龚彦晓), Zhenda Xie(谢臻达), Zhenlin Wang(王振林), and Shi-Ning Zhu(祝世宁)
Citation: Chin. Phys. B, 2025, 34 (**8**): 084205. DOI: 10.1088/1674-1056/adee8b
http://cpb.iphy.ac.cn; http://iopscience.iop.org/cpb

What follows is a list of articles you may be interested in

Reconfigurable microring resonators for multipurpose quantum light sources

Yuxing Du(杜昱星), Yingwen Liu(刘英文), Chao Wu(吴超), Pingyu Zhu(朱枰谕), Chang Zhao(赵畅), Miaomiao Yu(余苗苗), Yan Wang(王焱), Kaikai Zhang(张凯凯), and Ping Xu(徐平)
Chin. Phys. B, 2025, 34 (**7**): 074207. DOI: 10.1088/1674-1056/adcc88

Four-wave mixing Bragg scattering for small frequency shift from silicon coupled microrings

Chang Zhao(赵畅), Chao Wu(吴超), Pingyu Zhu(朱枰谕), Yuxing Du(杜昱星), Yan Wang(王焱), Miaomiao Yu(余苗苗), Kaikai Zhang(张凯凯), and Ping Xu(徐平)
Chin. Phys. B, 2025, 34 (**1**): 014206. DOI: 10.1088/1674-1056/ad8a4f

High-performance and fabrication friendly polarization demultiplexer

Huan Guan(关欢), Yang Liu(刘阳), and Zhiyong Li (李智勇)
Chin. Phys. B, 2022, 31 (**3**): 034203. DOI: 10.1088/1674-1056/ac21bc

Bandwidth-tunable silicon nitride microring resonators

Jiacheng Liu(刘嘉成), Chao Wu(吴超), Gongyu Xia(夏功榆), Qilin Zheng(郑骑林), Zhihong Zhu(朱志宏), and Ping Xu(徐平)
Chin. Phys. B, 2022, 31 (**1**): 014201. DOI: 10.1088/1674-1056/ac2e64

Highly sensitive digital optical sensor with large measurement range based on the dual-microring resonator with waveguide-coupled feedback

Xiang Xing-Ye (向星烨), Wang Kui-Ru (王葵如), Yuan Jin-Hui (苑金辉), Jin Bo-Yuan (晋博源), Sang Xin-Zhu (桑新柱), Yu Chong-Xiu (余重秀)
Chin. Phys. B, 2014, 23 (**3**): 034206. DOI: 10.1088/1674-1056/23/3/034206

RAPID COMMUNICATION

Euler-modified pulley-type microring on lithium niobate platform

Wen-Hui Song(宋文慧)[1,†], Dong-Jie Guo(郭东洁)[1,†], Ran Yang(杨然)[1], Jia-Chen Duan(端家晨)[1], Zi-Shuo Gu(顾子硕)[1], Ji Tang(汤济)[1,2], Zhilin Ye(叶志霖)[1,2], Xiao-Hui Tian(田晓慧)[1,‡], Kunpeng Jia(贾琨鹏)[1], Zhong Yan(严仲)[1], Zhijun Yin(尹志军)[2], Yan-Xiao Gong(龚彦晓)[1], Zhenda Xie(谢臻达)[1], Zhenlin Wang(王振林)[1], and Shi-Ning Zhu(祝世宁)[1]

[1] *National Laboratory of Solid State Microstructures, School of Physics, School of Electronic Science and Engineering, College of Engineering and Applied Sciences, and Collaborative Innovation Center of Advanced Microstructures, Nanjing University, Nanjing* 210093, *China*

[2] *NanZhi Institute of Advanced Optoelectronic Integration Technology Co., Ltd., Nanjing* 210093, *China*

(Received 18 April 2025; revised manuscript received 14 May 2025; accepted manuscript online 11 July 2025)

Microring resonators, as essential components of photonic integrated circuits, offer compact size, wavelength selectivity, and strong resonance effects, making them invaluable in optical computing, on-chip interconnects, and quantum photonics. The proposal of the pulley-type microring enhances the coupling strength, but also brings about issues such as mode mismatch and the excitation of higher-order modes. Here, a lithium niobate microring resonator coupled with a pulley bus waveguide based on modified Euler curves is proposed. This Euler-modified pulley bus minimizes mode mismatch at bending junctions, effectively suppressing higher-order mode excitation. The design achieves a high Q factor (exceeding 10^5) and strong coupling efficiency (83%) within a compact structure of 70 μm radius. Due to its simple structure and ease of fabrication, the Euler-modified pulley-type microring holds practical value for applications requiring high-quality microring resonators.

Keywords: photonic integrated circuits (PICs), microring resonators, lithium niobate on insulator (LNOI), Euler curve, single-mode excitation

PACS: 42.82.–m, 42.60.Da, 42.79.Gn

DOI: 10.1088/1674-1056/adee8b **CSTR:** 32038.14.CPB.adee8b

1. Introduction

In the era of information technology, photonic integrated circuits (PICs) are playing an increasingly important role,[1–3] finding widespread applications in quantum communication,[4,5] optical interconnects,[6,7] modulation,[8] biosensing,[9] and medical diagnostics.[10] Among various on-chip components, as critical building blocks in PICs, microring resonators[11,12] exhibit significant application potential in optical computing,[13] on-chip optical interconnects,[14,15] quantum optics,[16] quantum information processing,[17] and biosensing,[18] owing to their small footprint, excellent wavelength selectivity, and enhanced resonant field effects. To achieve optimal performance, microring resonators are typically required to possess a high quality factor (Q factor) to ensure narrow linewidths,[19] strong coupling to meet critical or over-coupling conditions,[20] and small footprint to enable a large free spectral range (FSR) and promote PIC miniaturization.[21]

Over the past decades, various microring resonator structures have been developed, including the single microring with a single bus waveguide,[22] the single microring with dual bus waveguides,[23] the racetrack-type resonator,[24] and the multiple microring configuration.[25] However, to realize high-density PICs, reducing the size of microrings is essential. A major drawback of these conventional designs lies in the huge bending or radiation losses from the microring, which results in decreased Q factors. To overcome these limitations, pulley-type microring structures[26–28] have been proposed and widely implemented to achieve high-Q microring resonators. In such structures, the bus waveguide wraps partially around the microring resonator, effectively extending the coupling length and enhancing the coupling strength. However, the curved sections of the pulley waveguide introduce mode mismatches at the transition regions, which lead to coupling losses and the excitation of higher-order modes. The lithium niobate on insulator (LNOI) platform,[29,30] with its high refractive index contrast, strong electro-optic effects, and tight integration capabilities, offers significant advantages for photonic integration. However, despite these benefits, challenges such as mode mismatch and coupling losses still persist. A common strategy to address these issues is to introduce a lateral offset between the incoming straight section and the bend.[31–33] Nonetheless, this approach demands extremely tight fabrication tolerances, and the problem of higher-order mode excitation remains unresolved. This limitation signifi-

[†]These authors contributed equally to this work.

[‡]Corresponding author. E-mail: tianxiaohui@nju.edu.cn

© 2025 Chinese Physical Society and IOP Publishing Ltd. All rights, including for text and data mining, AI training, and similar technologies, are reserved.

cantly restricts the performance of multimode microring resonators in applications requiring stable single-mode operation, such as self-injection-locked lasers and narrow-linewidth optical filters. The scattering resonances of higher-order modes can interfere with phase locking of the fundamental mode, thereby degrading overall device performance.

In this paper, we propose a microring resonator coupled with a modified Euler pulley bus waveguide, designed to address these issues by suppressing the excitation of higher-order modes through smooth transitions, while optimizing the performance of the microring resonator. The Euler curve provides a linear curvature transition from zero, enabling a gradual transformation of the modal field from the multimode straight waveguide to the multimode curved waveguide. This smooth transition at the microring bending interface reduces mode mismatch and suppresses higher-order mode excitation. To validate the feasibility of this coupler, we fabricated three types of lithium niobate microring resonators, including those coupled with circular pulley bus waveguides, Euler-modified pulley-type bus waveguides, and straight bus waveguides. Experimental results confirm that the Euler-modified pulley bus suppresses higher-order modes while significantly improving the intrinsic Q factor, exceeding 10^5. Moreover, the transmission of over-coupled microrings reaches 83%. Although the Q factor of this device is not particularly high compared to some of the currently known microring resonators, it achieves compatibility between low loss in our design and single-mode excitation through Euler curve geometry optimization, with a compact structure that also offers the advantages of functional integration. This compact multimode resonator with single-mode excitation holds great potential for the design of photonic integrated circuits, such as self-injection-locked lasers and high-performance filters, particularly in high-frequency applications that require low loss and compact structures.

2. Design

As shown in Fig. 1(a), a conventional circular pulley bus waveguide comprises three components: a central circular waveguide parallel to the microring to increase the coupling length, two straight waveguides connecting the microring to external devices, and two side circular waveguides connecting the initial curve to the straight waveguides. To attain a higher coupling strength, the widths of the waveguides should be carefully selected for phase matching between the bus and the ring waveguide. In this letter, we consider a 600-nm-thick X-cut LNOI with an etching depth of 300 nm, covered by a 1.5-μm-thick layer of silicon dioxide. The light propagates along the Y-axis in the straight waveguide. The radius of the microring R_0 is set to 70 μm to achieve a relatively large FSR of 300 GHz. The microring waveguide width W_0 is set to 1.5 μm to reduce scattering loss compared to a single-mode waveguide. The width of the bus waveguide W_b and the coupling gap g are carefully selected to be 1 μm and 700 nm, respectively, by calculating the phase factor ϕ between the microring and bus waveguides, where the propagation constants of the waveguide modes are simulated by mode solution. Furthermore, with the width of 1 μm, the bus waveguide is considered a single-mode waveguide that supports only the fundamental modes.

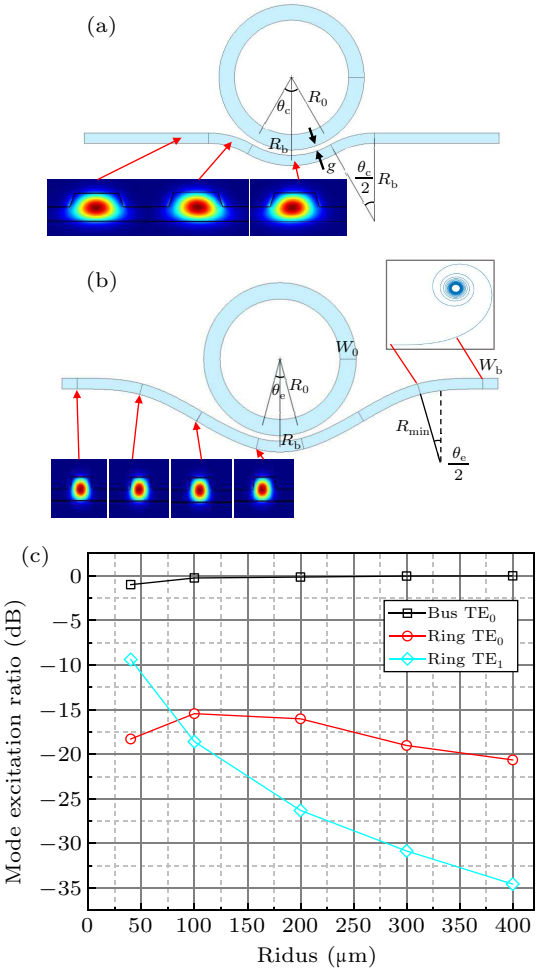


Fig. 1. Schematic configurations for microrings with circular (a) and Euler-modified (b) pulley bus. The inset of (a) is the TE_0 mode distribution of a straight waveguide and circular bends. The insets of (b) are respectively the TE_0 mode distribution at the waveguide interface and the diagram of the Euler curve. (c) Calculated mode excitation ratio from the bus TE_0 mode to engine modes in the coupled bus and ring structure.

Figure 1(a) demonstrates that the TE_0 mode distributions differ at the interfaces of the three constituent sections due to waveguide bending, indicating mode mismatch. To quantify mode mismatch, we simulate the mode excitation ratio (MER) at the circular bending interfaces, as shown in Fig. 1(c). As the radius of the circular waveguides decreases, the excitation ratio of the ring TE_1 mode increases. The demand for compact structures further exacerbates coupling losses and the undesired excitation of additional modes. To mitigate mode mismatch, the Euler bend[10,34] has been introduced as an effective solution. Here, we propose an Euler-modified pulley-type microring, as illustrated in Fig. 1(b). Two fully symmetric Euler

curve waveguides, each consisting of three identical modified Euler bends, replace the two side circular bend waveguides. As shown in the inset of Fig. 1(b), the Euler curve exhibits a curvature that increases linearly from zero along its length, ensuring a smooth transition at the microring bending interface. This gradual curvature variation facilitates the transformation of the modal field from the multimode straight waveguide to the low-loss multimode curved waveguide, effectively reducing mode mismatch and suppressing higher-order mode excitation. The Euler-modified pulley bus maintains mode consistency at the waveguide interface due to the gradual variation in curvature, in contrast to the mode discontinuities observed in the circular pulley bus. The minimum radius of the modified Euler bend $R_{\min}$ is the same as the radius of bus waveguide R_{b} to match the central circular waveguide. The central circular arcs of the circular and Euler-pulley bus are set to $\theta_{\mathrm{c}} = 15^{\circ}$ and $\theta_{\mathrm{e}} = 7.5^{\circ}$, respectively, to obtain approximate coupling strength. In the following text, we will refer to this entire segment of the waveguide as the Euler-modified pulley bus waveguide.

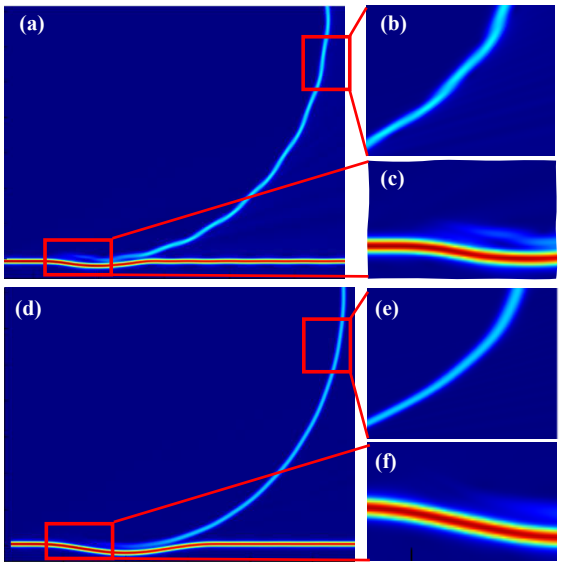


Fig. 2. The transmission results of light in the traditional pulley bus waveguide (a), Euler-modified pulley bus waveguide (b) coupled with a quarter ring. Panels (b) and (e) show the corresponding optical mode field distributions within the microring, while (c) and (f) present magnified views of the waveguide discontinuities.

To verify whether the Euler-modified pulley bus waveguide could suppress higher-order mode excitation, 3D-finite-difference time domain (FDTD) simulations are conducted. As shown in Figs. 2(a) and 2(d), light from the pulley bus waveguide couples into the ring waveguide. The sudden increase in the optical field in the ring waveguide at the junction (Fig. 2(c)), along with the oscillating light field in the circular bus structure (Fig. 2(b)) indicates higher-order mode excitation due to mode mismatch. In contrast, the Euler-modified pulley bus enables gradual light coupling into the ring without abrupt changes (Fig. 2(f)). Moreover, no interference fringes from multimode interactions are observed in Fig. 2(e), confirming the suppression of higher-order modes.

As we can see, the mode components of TE_1 are -17 dB (Fig. 3(a)) and -32 dB (Fig. 3(b)), respectively. The simulation results demonstrate that the Euler-modified pulley bus waveguide effectively suppresses the excitation of higher-order modes compared to the conventional pulley-type microring. Additionally, our analysis suggests that higher-order mode excitation may stem from mode discontinuities in the coupling waveguide. Even when the coupling waveguide does not support the TE_1 mode, it could still facilitate its excitation in the ring waveguide.

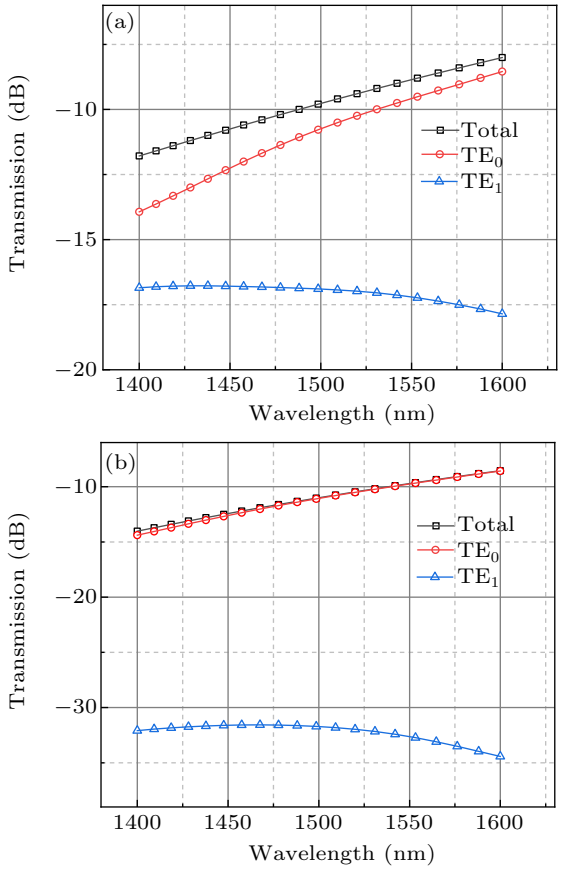


Fig. 3. Calculated transmissions from the TE_0 mode launched at the input straight waveguide of the circular pulley bus (a) and the Euler-modified pulley bus (b) to the modes in the microring bend.

3. Experiment

To experimentally demonstrate the viability of the scheme we proposed, relevant devices were fabricated and evaluated. Here, three types of rings are fabricated for comparison, including microrings coupled with circular pulley bus, Euler-modified pulley bus, and straight bus. The microring chips are fabricated by IOPTEE Inc. The waveguide structure is patterned by electron beam lithography (EBL) and transferred into the LN thin film via ion beam etching (IBE). Subsequently, a 1.5-μm-thick silica layer is deposited using plasma-enhanced chemical vapor deposition (PECVD). The optical images of three types of rings are shown in Fig. 4.

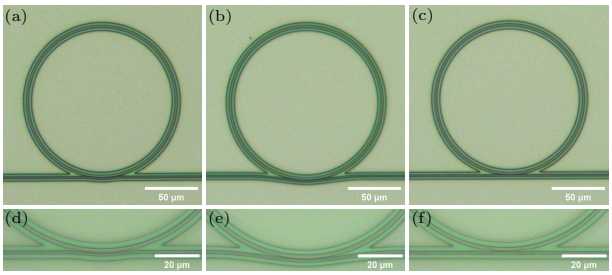


Fig. 4. Optical images of the microrings with (a) circular pulley bus, (b) Euler-modified pulley bus, and (c) straight bus. Panels (d)–(f) are the coupling regions of the three types of microrings, respectively.

Experimental procedure for microring characterization is illustrated in Fig. 5(a). We use a tunable semiconductor laser (Santec TSL-710) with a linewidth of 100 kHz and a scan speed of 20 nm/s, and the laser is coupled into the chip via a lensed fiber. At the output of the chip, a photodetector monitors the output power in real time, while a wavelength meter (HighFinesse WS-7) confirms the absolute wavelength. The measured transmission spectra of the three microrings near 1550 nm are shown in Figs. 5(b)–5(d). As shown in Fig. 5(b), both TE_0 and TE_1 modes are excited in the microring coupled with the circular pulley bus waveguide. In contrast, the spectra of the Euler-modified pulley bus structure (Fig. 5(c)) exhibit only TE_0 modes. Furthermore, a comparison was conducted with microrings coupled with straight waveguides (Fig. 5(d)), where higher-order modes were similarly not observed. Nevertheless, the straight waveguide configuration exhibits greater sensitivity to fabrication imperfections, leading to the persistent presence of the fundamental TM_0 mode across the entire spectral range. To further characterize the microring performance, the intrinsic Q factor (Q_0) and average transmission of the fabricated rings (12 of each type) are evaluated. The Euler-modified pulley bus microring exhibits the highest transmission (82%) with a Q_0 (8.66×10^5), comparable to the circular pulley bus microring (75% transmission, $Q_0 = 8.62 \times 10^5$). The straight bus microring shows the lowest values, with 71% transmission and a Q_0 of 7.29×10^5. Additionally, increasing θ in the Euler-modified pulley bus can enhance the coupling strength. With the phase matching condition satisfied, the coupling strength can achieve 100%, theoretically.

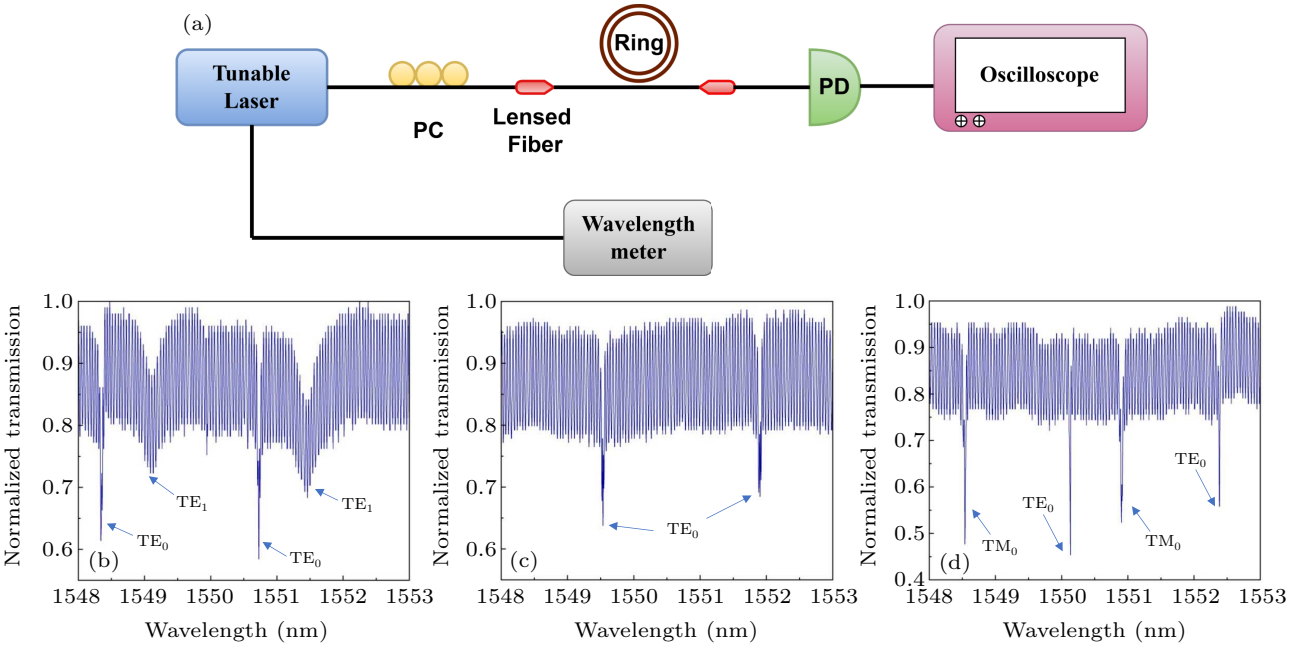


Fig. 5. Measurement setup and separate characterizations of microring. (a) Schematic drawing of the measurement setup. Transmission spectra of the microring with circular pulley bus (b), Euler-modified pulley bus (c), and straight bus (d).

4. Conclusion

In conclusion, we have demonstrated a strong overcoupled multi-mode lithium niobate microring resonator with single-mode excitation by utilizing an Euler-modified pulley bus. The mode mismatch in the circular pulley bus is analyzed, and the high-order mode excitation in the Euler-modified pulley configurations is simulated using 3D FDTD. To validate the simulations, we fabricate three types of microrings: circular pulley bus, Euler-modified pulley bus, and straight bus. The Euler-modified pulley bus, through a curvature gradient design (with curvature increasing linearly from zero), achieves a smooth mode field transition, reducing the excitation of higher-order modes to negligible levels. This enables single-mode excitation in the compact pulley-type microring, while maintaining a high Q factor and strong coupling efficiency. While the Q factor is slightly lower than that of some reported microring resonators, it achieves compatibility between low-loss and single-mode excitation through Euler curve geometry optimization, offering functional integration advantages within a compact structure. Combined with the increasing fab-

rication difficulties, this design is highly valuable for many devices requiring low loss, compact microring with a pure transmission spectrum, such as self-injection locking lasers, broadband filters, and compact phase modulators.

Acknowledgments

Project supported by the National Key Research and Development Program of China (Grant No. 2024YFB2808300), the National Natural Science Foundation of China (Grant Nos. 62293523, 62288101, 62305156, 92463304, 92463308, 12304421, and 12341403), Zhangjiang Laboratory (Grant No. ZJSP21A001), Program of Jiangsu Natural Science Foundation (Grant Nos. BK20230770 and BK20232033), and Guangdong Major Project of Basic and Applied Basic Research (Grant No. 2020B0301030009).

References

[1] Vlasov Y A and McNab S J 2004 *Opt. Express* **12** 1622
[2] Lin J T, Bo F, Cheng Y and Xu J J 2020 *Photonics Res.* **8** 1910
[3] Qi Y F and Li Y 2020 *Nanophotonics* **9** 1287
[4] Dorin B A and Ye W N 2014 *Opt. Express* **22** 4547
[5] Pelucchi E, Fagas G, Aharonovich I, Englund D, Figueroa E, Gong Q H, Hannes H, Liu J, Lu C Y, Matsuda N, Pan J W, Schreck F, Sciarrino F, Silberhorn C, Wang J W and Jöns K D 2022 *Nat. Rev. Phys.* **4** 194
[6] Li S Y, Zhou Y Y, Dong J J, Zhang X L, Cassan E, Hou J, Yang C Y,Chen S P, Gao D S and Chen H Y 2018 *Optica* **5** 1549
[7] Seok T J, Kwon K, Henriksson J, Luo J H and Wu M C 2019 *Optica* **6** 490
[8] Chiles J and Fathpour S 2014 *Optica* **1** 350
[9] Li G L, Yao J, Thacker H, Mekis A, Zheng X Z, Shubin I, Luo Y, Lee J H, Raj K, Cunningham J E and Krishnamoorthy A V 2012 *Opt. Express* **20** 12035
[10] Cherchi M, Ylinen S, Harjanne M, Kapulainen M and Aalto T 2013 *Opt. Express* **21** 17814
[11] Van V 2016 *Optical Microring Resonators: Theory, Techniques, and Applications* (Boca Raton, FL: CRC Press)
[12] Bogaerts W, De Heyn P, Van Vaerenbergh T, De Vos K, Kumar Selvaraja S, Claes T, Dumon P, Bienstman P, Van Thourhout D and Baets R 2012 *Laser Photonics Rev.* **6** 47
[13] Qiu C Y, Xiao H F, Wang L H and Tian Y H 2022 *Front. Optoelectron.* **15** 1
[14] Xu Q F, Schmidt B, Shakya J and Lipson M 2006 *Opt. Express* **14** 9431
[15] Liu J C, Xia G Y, Hong Q, Zhu P Y, Zhang K K, Xia K Y, Xu P, Qin S Q and Zhu Z H 2024 *Chin. Phys. B* **34** 034204
[16] Su X, Jin B B, Tang J S and Xia K Y 2024 *Chin. Phys. B* **41** 074202
[17] Xu L, Wang L X, Chen G J, Chen L, Yang Y H, Xu X B, Liu A P, Li C F, Guo G C, Zou C L and Xiang G Y 2023 *Chin. Phys. B* **40** 093701
[18] Sun Y Z and Fan X D 2011 *Anal. Bioanal. Chem.* **399** 205
[19] Zhang M, Wang C, Cheng R, Shams-Ansari A and Lončar M 2017 *Optica* **4** 1536
[20] Liang G Z, Huang H Q, Mohanty A, Shin M C, Ji X C, Carter M J, Shrestha S, Lipson M and Yu N F 2021 *Nat. Photonics* **15** 908
[21] Chen L, Sherwood-Droz N and Lipson M 2007 *Opt. Lett.* **32** 3361
[22] Terrel M, Digonnet M J F and Fan S H 2009 *Laser Photonics Rev.* **3** 452
[23] Nawrocka M S, Liu T, Wang X and Panepucci R R 2006 *Appl. Phys. Lett.* **89** 071110
[24] Menon V M, Tong W and Forrest S R 2004 *IEEE Photonics Technol. Lett.* **16** 1343
[25] Poon J K S, Scheuer J, Xu Y and Yariv A 2004 *J. Opt. Soc. Am. B* **21** 1665
[26] Hosseini E S, Yegnanarayanan S, Atabaki A H, Soltani M and Adibi A 2010 *Opt. Express* **18** 2127
[27] Xie J Y, Zhou L J, Sun X M, Zou Z, Lu L J, Zhu H K, Li X W and Chen J P 2014 *Appl. Opt.* **53** 878
[28] Cai D P, Lu J H, Chen C C, Lee C C, Lin C E and Yen T J 2017 *Sci. Rep.* **5** 10078
[29] Zhu D, Shao L B, Yu M J, Cheng R, Desiatov B, Xin C J, Hu Y W, Holzgrafe J, Ghosh S, Shams-Ansari A, Puma E, Sinclair N, Reimer C, Zhang M and Loněar M 2021 *Adv. Opt. Photonics* **13** 242
[30] Honardoost A, Abdelsalam K and Fathpour S 2020 *Laser Photonics Rev.***14** 2000088
[31] Kitoh T, Takato N, Yasu M and Kawachi M 1995 *J. Lightwave Technol.* **13** 555
[32] Yen M H, Feng P Y, Lin C E, Chen C C and Chang J Y 2018 *Micromachines* **9** 226
[33] Fujisawa T, Makino S, Sato T and Saitoh K 2017 *Opt. Express* **25** 9150
[34] Jiang X H, Wu H and Dai D X 2018 *Opt. Express* **26** 17680